NJC

Cite this: *New J. Chem.*, 2011, **35**, 2356–2365

www.rsc.org/njc

PAPER

The role of the dendritic support in the catalytic performance of peripheral pincer Pd-complexes†‡

Niels J. M. Pijnenburg,[a] Martin Lutz,[b] Maxime A. Siegler,[b] Anthony Spek,[b] Gerard van Koten[a] and Robertus J. M. Klein Gebbink*[a]

Received (in Montpellier, France) 26th April 2011, Accepted 27th June 2011
DOI: 10.1039/c1nj20366e

To investigate the effects of the dendrimer backbone on catalysis, a series of monomeric and dendritic SCS-pincer Pd-complexes was synthesized and tested in two different Pd(II)-catalyzed reactions. To this end, the three novel polar PAMAM dendrimer-immobilized SCS-pincer Pd-complexes **3**, **4**, and **5**, and the two apolar carbosilane dendrimer-immobilized complexes **7** and **8** were compared to three monomeric analogues **1**, **2** and **6**. These complexes were investigated in the cross-coupling reaction between vinyl epoxide and styrylboronic acid and the auto-tandem reaction of cinnamyl chloride, hexamethylditin, and 4-nitrobenzaldehyde. The differences in catalytic rate and product selectivity for these complexes are described and discussed. For the cross coupling reaction, the PAMAM dendrimer-immobilized complexes were found to give a similar reaction rate, but a higher product selectivity than their monomeric counterparts. The carbosilane complexes showed a lower reaction rate and similar product selectivity. These observations are explained in view of dendrimer aggregation and peripheral group backfolding.

Introduction

Dendrimer-immobilized catalysts combine the benefits of homogeneous catalysis, namely high activity, tunable solublility, a well-understood catalyst description and mild reaction conditions, with the key benefit of heterogeneous catalysis: the recyclability of the catalyst.[1] Since the first report appeared by van Koten and van Leeuwen,[2] the field of dendrimer-immobilized catalysts has expanded enormously. Several comprehensive reviews have been published that provide an overview on dendrimer-immobilized organometallic catalysts, thereby focusing on the recyclability and the differences of these dendritic catalysts in terms of reaction rate and/or selectivity compared to their monomeric, non-dendritic counterparts.[3–8]

Most dendritic catalysts consist either of a single catalytic unit connected to the focal point of a dendritic wedge to increase steric bulk around the reaction center, or of multiple catalytic units that are connected to the periphery of a dendritic support. The role of the dendritic support on the overall catalytic performance of both types of dendritic catalysts is not negligible.[9] Except for electronic effects that may result from the covalent connection of the dendrimers to the organometallic catalyst, steric effects seem to play a more pronounced role. In close proximity of the dendritic backbone, the chemical micro-environment near the catalytic center may significantly alter.[10] Limited accessibility due to additional steric bulk around a catalytic center might impede substrate binding and therefore is an important reason for dendritic effects to be observed on catalytic reaction rates or product selectivities.

Several examples that reveal positive dendritic effects in terms of a higher product selectivity for dendritic catalysts in comparison to non-dendritic catalysts have been reported.[11–15] In these cases the increased steric crowding around the catalytic reaction center seems to hamper the formation of sterically unfavored (often branched) isomers in favor of less sterically demanding (often linear) isomers, thus improving the selectivity. Positive dendritic effects on reaction rate and product yield have also been observed.[16–20]

The origins of these effects are diverse. For example, in a recent paper Snelders *et al.* observed that higher generations of oligocationic dendritic ligands can stabilize the mono-ligated active species in the Suzuki–Miyaura cross-coupling reaction of aryl chlorides with phenyl boronic acids.[18] On the other hand, cooperation between two or multiple catalytic centers might be favored in the case of peripherally immobilized catalysts. Jacobsen *et al.* reported a positive effect for the Co–salen catalyzed hydrolytic kinetic resolution of epoxides,

[a] *Organic Chemistry & Catalysis, Debye Institute for Nanomaterials Science, Utrecht University, Universiteitsweg 99, 3584 CG Utrecht, The Netherlands. E-mail: r.j.m.kleingebbink@uu.nl; Fax: +31-30-252-3615*
[b] *Crystal and Structural Chemistry, Bijvoet Center for Biomolecular Research, Utrecht University, Padualaan 8, 3584 CH Utrecht, The Netherlands*

† Dedicated to Prof. Didier Astruc on the occasion of his 65th birthday.
‡ Electronic supplementary information (ESI) available. CCDC reference numbers 824226, 824227, 824228. For ESI and crystallographic data in CIF or other electronic format see DOI: 10.1039/c1nj20366e

a reaction known to be second order in Co.[20] The Kharasch addition, an atom transfer radical reaction, performed by immobilized NCN-pincer nickel catalysts by Kleij *et al.* is another example, although this has led to a negative dendritic effect.[19]

The choice of the type of dendritic support used for the dendrimer immobilization of a catalyst is often not specifically stated, and sometimes even seems quite randomly chosen. Experience in the research group, dendrimer availability and price, rather than arguments based on chemical properties are often important parameters for the selection of the dendritic support used for catalyst immobilization. As a result, only few reports detail the specific effects of the use of a different dendrimer support on one and the same reaction catalyzed by identical catalytic sites.[15,21] In addition, obtaining a balanced overview of such effects by combining data from different literature reports is difficult. For these reasons, we set out to study the catalytic performance of dendrimer-immobilized catalysts by maintaining a single catalyst type and instead changing the dendritic support.

In this study, two abundantly used but chemically different types of dendrimers have been used as supports for catalyst immobilization: polyamidoamine (PAMAM) dendrimers and carbosilane (CS) dendrimers.[22] PAMAM dendrimers are possibly the most frequently used types of dendrimers in materials science, biotechnology applications and catalysis and are commercially available. These polar dendrimers consist of an ethylenediamine core that has been reacted through a divergent synthesis protocol with methyl acrylate and ethylenediamine to create higher generations of dendrimers.[23–25] Carbosilane dendrimers on the other hand are apolar dendrimers that consist of C–Si and C–C bonds. The central silicon atom and other peripheral silicon centers act as the branching points in these dendrimers. Because of their chemical inertness these dendrimers are often used in catalysis.[26,27] Carbosilane dendrimers are usually synthesized in a divergent manner in an iterative two-step protocol using alternate allylation and hydrosilylation steps.[28]

We have studied two SCS-pincer Pd-catalyzed reactions with a series of different SCS-pincer Pd-catalysts. This series consist of the 'parent' SCS-pincer Pd-complex **1**, two monomeric *para*-substituted SCS-pincer Pd-complexes (**2** and **6**) as models for the dendrimer supported complexes, and a series of PAMAM (**3–5**) and CS (**7** and **8**) dendrimer-supported pincer Pd-complexes (Fig. 1).

This series of eight different SCS-pincer Pd-complexes was tested in two different Pd-catalyzed reactions: (1) the cross coupling of vinyl epoxide with phenylvinylboronic acid,[29] and (2) an auto-tandem reaction consisting of the stannylation of cinnamyl chloride followed by allylation of 4-nitrobenzaldehyde resulting in functionalized allylic alcohols (Fig. 2).[30] In both reactions, different reaction products can be formed; either a linear/branched or a *syn*/*anti* product mixture. In this way, not only the catalytic reaction rate, but also the product profile

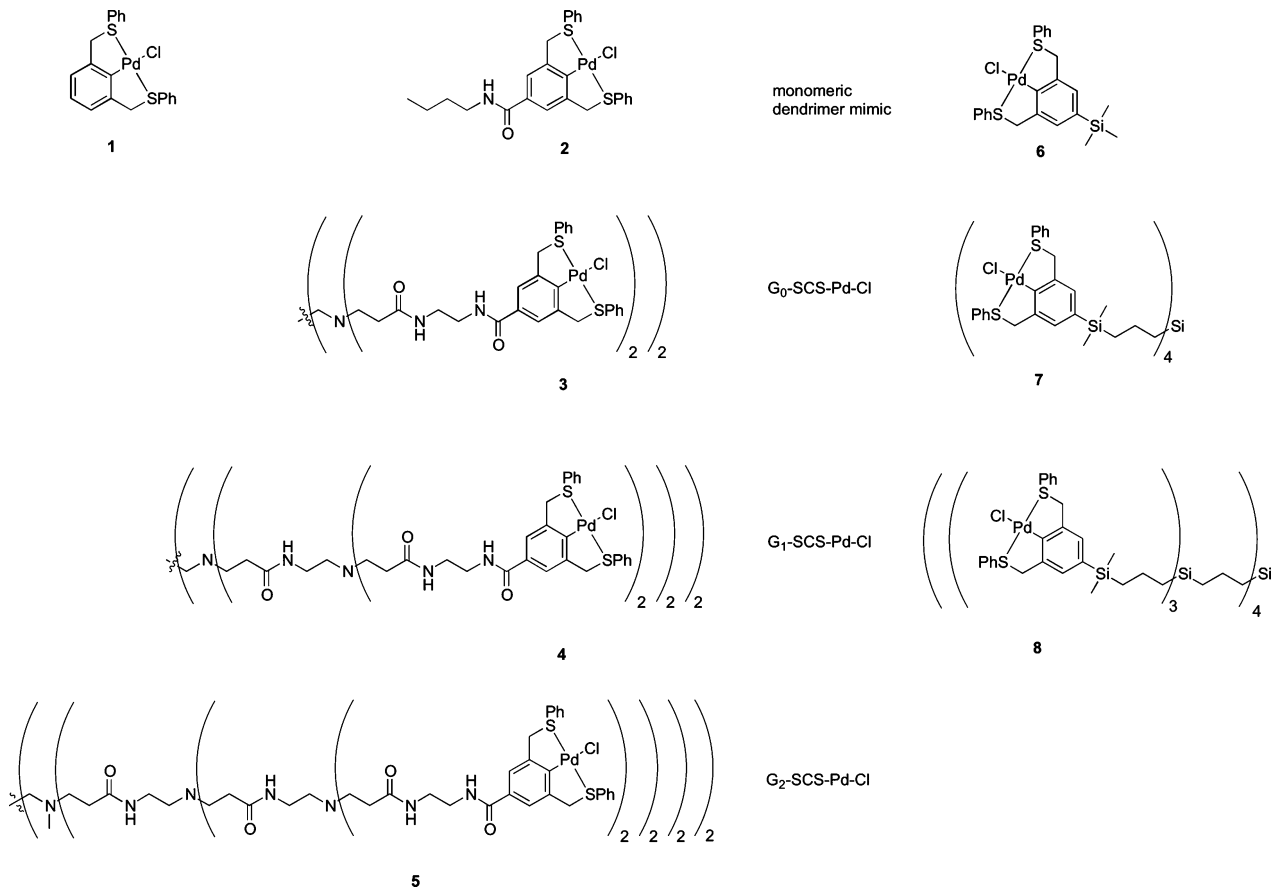

Fig. 1 Monomeric and dendritic SCS-pincer Pd-complexes **1–8** comprising either PAMAM or carbosilane dendritic scaffolds.

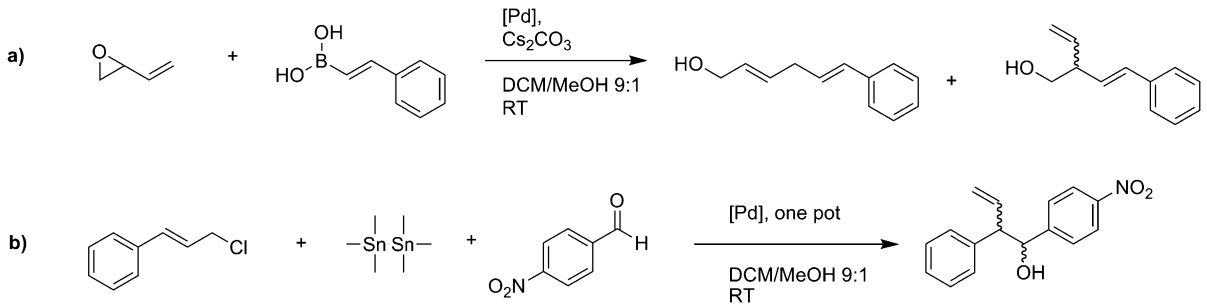

Fig. 2 SCS-pincer Pd-catalyzed reactions: (a) cross coupling between vinyl epoxide and styrylboronic acid, and (b) auto-tandem reaction between cinnamyl chloride, hexamethylditin, and 4-nitrobenzaldehyde.

can be used to parameterize the effect of the dendritic supporting scaffold on the performance of the SCS-pincer Pd-catalysts.

Results and discussion

Synthesis and analysis of SCS-pincer Pd-complexes

Synthesis. Monomeric pincer complex **2** and dendritic pincer complexes **3–5** were synthesized *via* an amide coupling between a primary amine (*i.e.* *n*-butylamine or commercially available amino-terminated PAMAM dendrimers) and an activated ester pincer derivative. This coupling reaction is based on an earlier reported protocol in which an NCN-Pd-pincer active ester compound was used to connect NCN-pincer Pd-complexes to various amines *via* a robust amide linkage.[31]

The activated ester functionalized SCS-pincer Pd-complex **13** was synthesized starting from commercially available 1-bromo-3,5-dimethylbenzene (Fig. 3). Bromination of this xylene *via* a light-induced reaction using *N*-bromosuccinimide (NBS) in methyl acetate, prevents the use of the more commonly published, but very environmentally unfriendly NBS bromination in carbon tetrachloride.[32] The resulting 1-bromo-3,5-bis(bromomethyl)benzene **9** was reacted under basic conditions with thiophenol to yield SCS-pincer preligand **10**.[33] Subsequently, ligand **10** was lithiated upon addition of two equivalents of *t*BuLi at −80 °C in diethylether. Quenching of this mixture by addition of (gaseous) carbon dioxide at −80 °C,[34] and protonation by addition of water lead to carboxylic acid **11** in 71% yield. This amphiphilic compound is hardly soluble in organic solvents, therefore the next synthetic step was performed in suspension. EDC coupling (EDC = 1-ethyl-3-(3-dimethylamino-propyl)carbodiimide; a water soluble carbodiimide) of **11** with *N*-hydroxysuccinimide in the presence of triethylamine yielded active ester **12** in good yields. Palladation of **12** was carried out using $[Pd(MeCN)_4](BF_4)_2$ in refluxing acetonitrile. After treatment of the resulting cationic SCS-pincer Pd–NCMe complex with sodium chloride for 1 h, the resulting *para*-succinimidyl ester functionalized SCS-pincer Pd-complex **13** was isolated as an air-stable yellow powder.

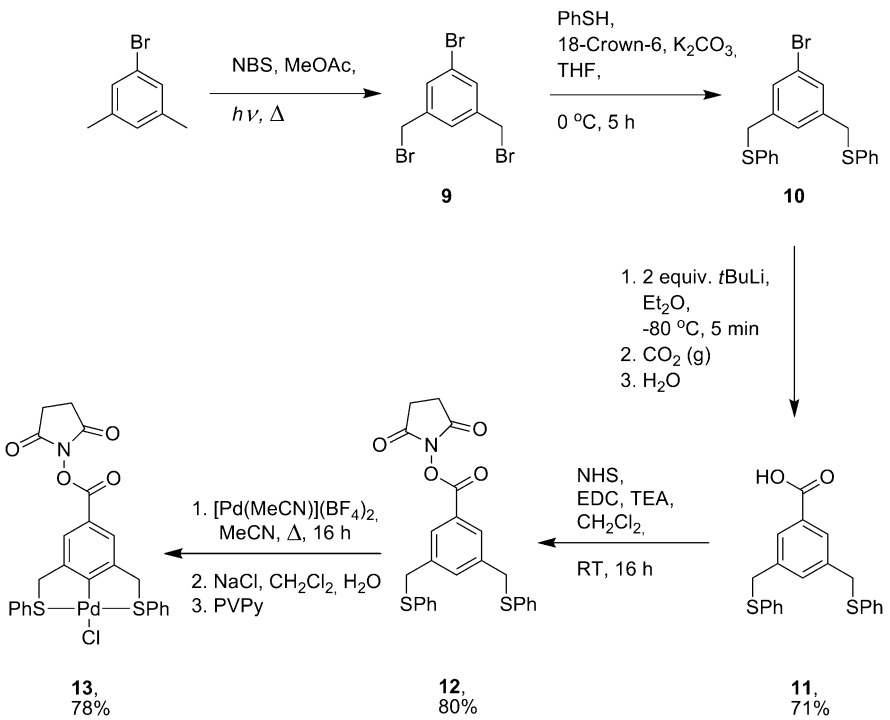

Fig. 3 Synthesis of succinimidyl ester functionalized SCS-pincer Pd-complex **13**.

In a last step, a solution of **13** was treated with 100 equivalents of crosslinked (polyvinyl)pyridine (PVPy) for 3 h. This last step was performed to chelate Pd(0) particles that might still be present as byproducts after the introduction of the palladium centers.[35] These particles could potentially lead to undesired competition in catalysis, therefore care was taken to avoid these particles in the final batch of **13**. After treatment with PVPy beads, active ester SCS-pincer complex **13** was obtained in 78% yield as a pale yellow powder.

Next, compound **13** was used to couple SCS-pincer Pd-complexes to primary amines in dichloromethane or in a mixture of dichloromethane and methanol under ambient conditions (Fig. 4). The latter solvent was used to improve the solubility of the dendritic products. As it turned out, **13** did not undergo nucleophilic substitution by methanol under these conditions. Using *n*-butylamine as nucleophile leads to monomeric complex **2** in 82% yield. Succinimidyl ester **13** was connected in the same way to the peripheral groups of commercially available PAMAM dendrimers leading to dendritic complexes **3–5**. A slight excess of 1.25 equivalents of pincer complex **13** per dendritic arm was used in this protocol. The resulting dendritic complexes were purified from the succinimide byproduct *via* passive dialysis and the dendritic products were isolated in good yields (66–78%) as yellow powders. The solubility of these dendrimers is not very high in most common organic solvents. Polar aprotic solvents like DMF and DMSO and a mixture of dichloromethane and methanol are solvents in which these complexes showed good solubility. These dendritic catalysts were neither soluble in pure dichloromethane nor in pure methanol.

The synthesis of *para*-TMS SCS-pincer Pd-complex **6** and carbosilane dendrimers **7** and **8** has been published earlier by us,[35] and will not be detailed here.

Analysis of PAMAM dendrimers 3, 4 and 5. To get insight in the integrity and catalyst loading of dendritic complexes **3–5**, a variety of analytical techniques have been applied. The smallest PAMAM dendrimer complex, *i.e.* G_0 compound **3**, was successfully characterized by ESI-MS. Signals contributed to the $[M - 2Cl]^{2+}$ fragment with m/z = 1201.0618 (calc. m/z = 1201.0865) and to the $[M - 3Cl + Na + x\text{MeCN}]^{2+}$ (x = 2–4) fragments were identified. For the higher generation dendritic compounds **4** and **5**, no correct mass spectra could be obtained. Due to their macroscopic size these compounds could not be detected either by ESI-MS or by MALDI-TOF MS.

Proton and carbon NMR analysis showed shifts of the signals of the most peripheral CH_2 groups of the PAMAM dendrimer after coupling (^{1}H NMR: from 2.8 ppm to 3.4 ppm; ^{13}C NMR from 41 ppm to 39 ppm). Nearly identically IR spectra for **3**, **4**, and **5**, together with negative ninhydrin tests[36] performed after the coupling reaction of succinimidyl ester functionalized SCS-pincer Pd-complex **13** with the G_x-PAMAM-NH_2 dendrimers, hinting at the absence of primary amine groups, conclude that for all generations PAMAM dendrimers a complete coupling reaction has taken place leading to fully metallated dendrimers **3–5**.

Catalytic results

Cross coupling of vinyl epoxide with phenylvinylboronic acid. The ECE-pincer Pd-catalyzed cross coupling of vinyl epoxides with boronic acids (reaction (1), Fig. 2) has been introduced by Kjellgren *et al.*[29] and has been studied in a later stage by Bonnet using SCS-pincer Pd-complexes.[37] This reaction allows for a range of vinyl epoxides to be coupled to various boronic acids using NCN-, SCS- and SeCSe-pincer Pd–Cl complexes. These reactions proceed *via* either an S_N2 or S_N2' mechanism and lead to a mixture of linear and branched products in a ratio of 2.3 for $N^{Me}CN^{Me}$-pincer Pd-complexes[29] and 3.8 for $S^{iPr}CS^{iPr}$-pincer Pd-complexes.[37]

The dendritic catalysts **3**, **4**, and **5** do not dissolve in the THF/water mixture used by Kjellgren[29] and Bonnet.[37] For this reason, a mixture of CH_2Cl_2/MeOH (9 : 1 v/v) was used for the catalytic tests; in this solvent mixture the reaction substrates and catalysts are fully soluble, and reproducible catalytic results were obtained. In the reaction setup, two

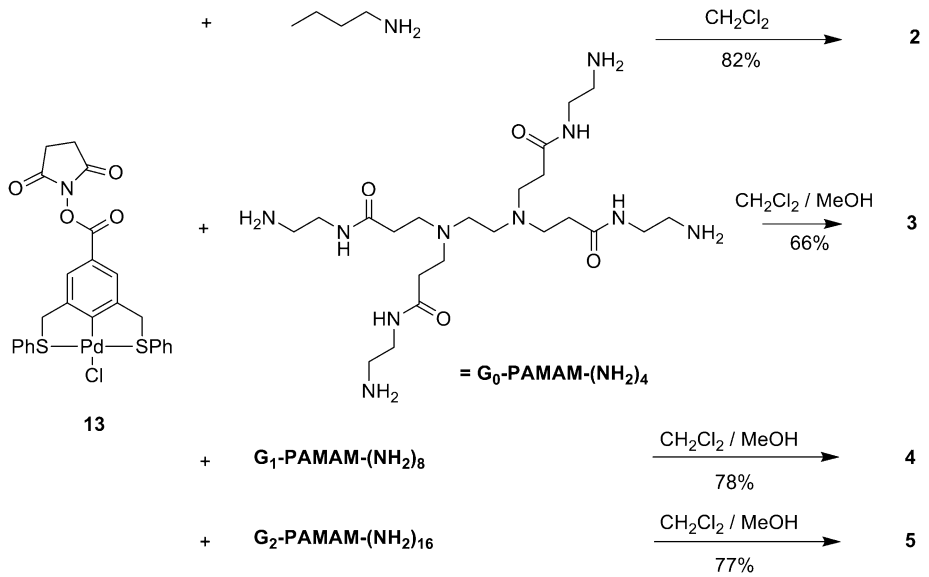

Fig. 4 Synthesis of monomeric complex **2** and dendritic complexes **3–5** by active ester chemistry.

equivalents of caesium carbonate were used as base and 2 mol% of Pd were used as catalyst in 2 mL CH_2Cl_2/MeOH. The linear product 6-phenylhexa-2,5-dien-1-ol and the branched product 4-phenyl-2-vinylbut-3-en-1-ol were observed as major reaction products. In addition, fractions of styrene (hydrolysis product) and 1,4-diphenylbuta-1,3-diene (homocoupling product) were found. After 3 h of reaction time, the formation of 60–63% cross coupling products, 34–38% styrene, and 2–3% 1,4-diphenylbuta-1,3-diene were typically found for all tested catalysts. The amount of hydrolysis product that was found is higher than reported in the literature,[29] and is likely caused by the change of the reaction medium from THF/H_2O to CH_2Cl_2/MeOH. Without catalyst (blank reaction) no product formation was observed.

The conversion of phenylvinylboronic acid in reaction (1) in time catalyzed by the different SCS-pincer Pd-complexes is depicted in Fig. 5a–c for the PAMAM-based catalysts **1–5**, for the series of carbosilane dendrimers **1** and **6–8**, and for the respective G0 and G1 PAMAM and CS dendrimers. Furthermore, the ratio between linear and branched cross-coupling product is shown in Fig. 5d for all catalysts.

In this particular reaction, the effect of both the presence and the absence of a PAMAM-scaffold on the reaction rate appears to be minimal (Fig. 5a). For all tested generations of PAMAM dendrimers (catalysts **3–5**) and for monomeric catalyst **2** the observed overall reaction rates are identical, and somewhat lower than for parent catalyst **1**. Dendrimers **4** and **5** did show a somewhat higher conversion after 30 minutes, but this difference was cancelled out after about 1 h. The linear/branched selectivity increases significantly from 5.5–6.0 for the monometallic catalysts **1** and **2** to 7.0–8.5 for the dendritic PAMAM catalysts **3**, **4** and **5** (Fig. 5d). There seems to be no direct relation with the size of the dendrimer or the number of SCS-pincer Pd-units per dendrimer and the observed *l*/*b* ratio, as this ratio increases from **2** to **3** (6.0 and 8.2 respectively), then decreases again for **4**, and reaches a maximum of 8.4 for **5**. Amongst these catalysts, monomeric catalyst **2** shows the lowest *l*/*b* ratio, which hints at a positive influence of the dendritic catalyst structure on the *l*/*b* ratio.

Carbosilane dendrimers **7** and **8** showed a somewhat higher initial reaction rate than the monomeric catalysts **1** and **6**. However, after 1 h the monomeric catalysts are significantly faster than dendritic catalysts **7** and **8**. These dendritic catalysts showed a different overall reaction profile than all other catalysts tested here. While the other catalysts displayed a fairly S-type reaction profile, catalysts **7** and **8** showed a more linear reaction profile in which the overall reaction rate considerably dropped compared to monomeric catalysts **1** and **6** (Fig. 5b). The *l*/*b* selectivity for catalysts **1**, **6**, **7**, and **8** showed only small differences and all appeared close to the observed ratio for parent catalysts **1** of 5.5. TMS-appended catalyst **6** showed in fact the highest *l*/*b* selectivity (5.9) amongst the carbosilane series. The selectivity decreases for **7** to 4.9 and then increases back for **8** close to the selectivity of **6**.

When the catalytic performance of the polar PAMAM dendrimers **3** and **4** was compared to the apolar carbosilane dendrimers **7** and **8**, the PAMAM dendrimers were found to be superior by showing a higher reaction rate and a higher *l*/*b* ratio (Fig. 5c + d).

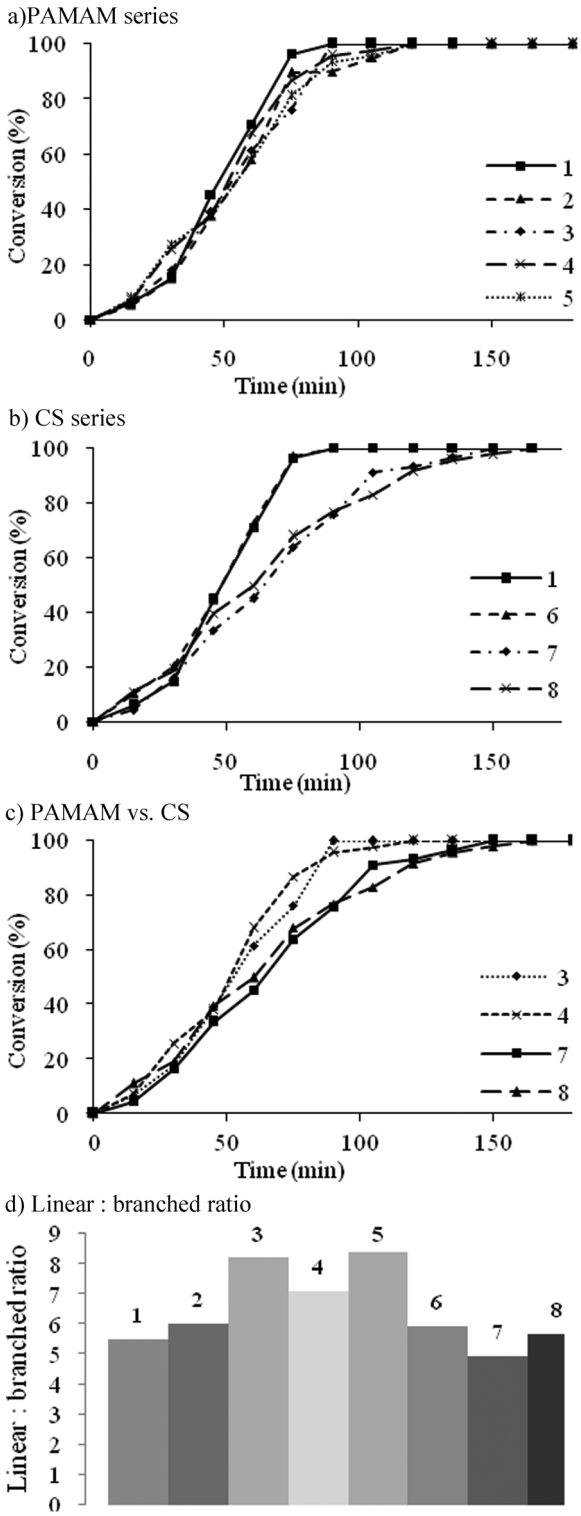

Fig. 5 (a, b, c) Conversion of phenylvinylboronic acid in the SCS-pincer Pd-complex catalyzed cross coupling with vinyl epoxide at constant Pd-concentration. (d) Linear/branched product ratio of this coupling using different SCS-pincer Pd-complexes.

Tandem catalysis. Next, the dendritic catalysts were tested in auto-tandem reaction 2 (Fig. 2). These catalysts were tested both in solution and in a compartmentalized setup using membrane dialysis bags.[35] Starting from a mixture of the three

reaction substrates cinnamyl chloride, hexamethylditin and 4-nitrobenzaldehyde, a mixture of stereoisomers of the 1-(4-nitrophenyl)-2-phenylbut-3-en-1-ol product was obtained. The ratio of *anti* (*RS* and *SR*) and *syn* (*RR* and *SS*) products depends on the particular catalyst that is used in the reaction.

In these experiments, three equivalents of cinnamyl chloride and hexamethylditin were used with respect to the amount of 4-nitrobenzaldehyde. These substrate ratios were used because earlier studies have shown that only under these conditions the tandem reaction operates through a Pd(II) cycle and that the formation and participation of Pd(0) is excluded.[38] Again, a mixture of CH_2Cl_2 and MeOH (9 : 1 v/v) has been used as solvent system and no reaction was observed in the absence of catalysts.

Fig. 6 depicts the conversion of the cinnamyl chloride substrate using the eight different SCS-pincer palladium complexes **1–8**. The conversion of this substrate appeared to be almost independent of the catalyst used (Fig. 6a–c). In all cases, the conversion of cinnamyl chloride is complete within 2 h and all kinetic curves seemingly follow a first order type reaction profile. Amongst the dendritic catalysts, G_0-PAMAM dendrimer **3** seems to be the most active one (Fig. 6c). Also for the second step in this tandem reaction (*i.e.* the formation of the reaction product 1-(4-nitrophenyl)-2-phenylbut-3-en-1-ol) all eight tested catalysts, whether monomeric, dendritic, polar or apolar, showed very similar reaction profiles. The *anti*/*syn* ratio of the tandem products appeared to be between 1.4 and 1.5 for all catalysts (Fig. 6d). Exceptions are monomeric catalyst **2** that showed a slightly higher *anti*/*syn* ratio of 1.6 and the PAMAM G2 catalyst **5** that showed a significantly higher *anti*/*syn* ratio of 1.9.

Discussion and conclusion

In this paper two series of dendritic catalysts were studied: one series is based on the polar PAMAM scaffold (catalysts **3–5**) and the other series on the apolar CS scaffold (catalysts **7–8**). Together with monomeric catalysts **1**, **2** and **6**, which are the parent catalyst **1** and two monometallic catalysts that are electronically equivalent to the PAMAM-based (catalyst **2**) and the CS-based catalysts (catalyst **6**), these dendritic catalysts have been tested in two different Pd-catalyzed reaction to investigate whether the dendritic support itself plays a role in the catalytic parameters of these reactions.

For the Pd-catalyzed cross coupling of vinyl epoxide with phenylvinylboronic acid (reaction 1) small but significant rate and selectivity differences between monomeric catalysts, polar PAMAM and apolar CS dendritic catalysts have been found. Because the three monomeric catalysts **1**, **2** and **6** showed very similar characteristics for this reaction, these differences are not caused by remote electronic effects on the catalytic center, but rather by steric effects. The PAMAM-based dendritic catalysts showed a very similar reaction rate compared to the monomeric catalysts, while the carbosilane-based dendritic catalysts were found to be considerably slower than their monomeric counterparts. The product selectivity in this cross-coupling reaction showed another trend. Here, the monomeric catalysts and the carbosilane dendrimers showed a linear/branched product ratio around 5–6, whereas the PAMAM dendrimers showed a noticeably higher *l*/*b* ratio of 8–9: a small, but significant positive dendritic effect.

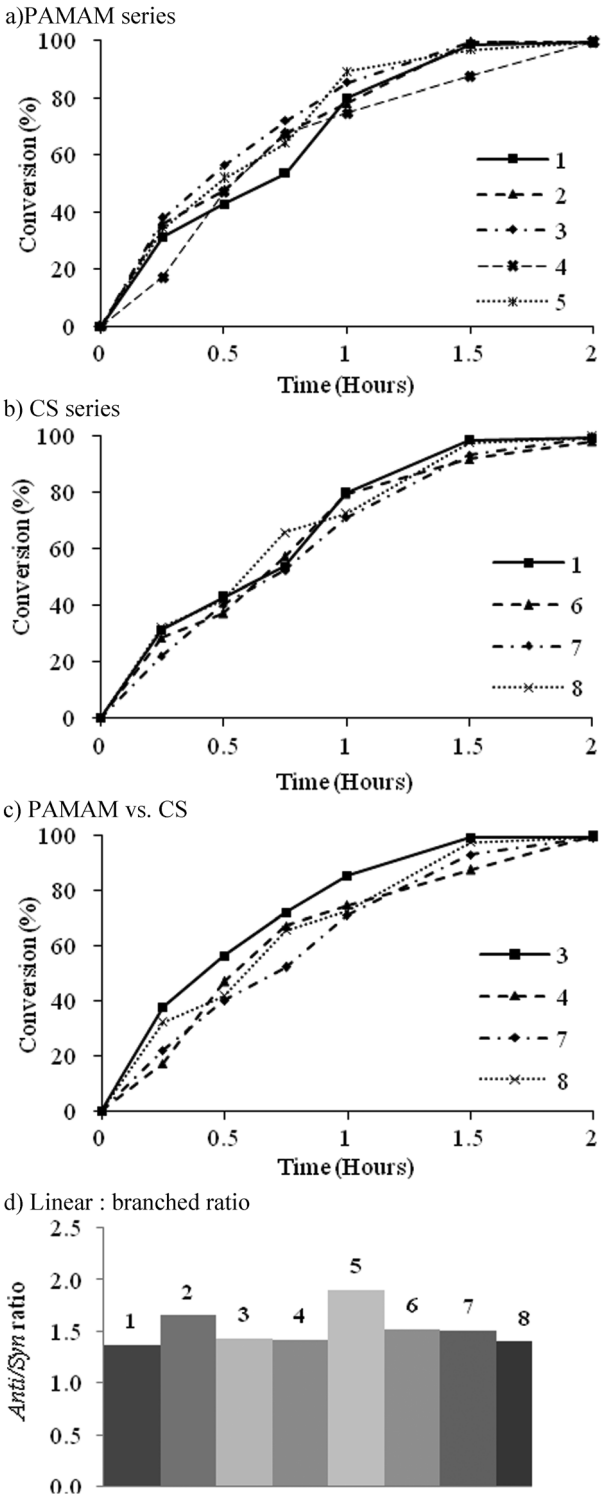

Fig. 6 (a, b, c) Conversion of cinnamyl chloride in the SCS-pincer Pd-complex catalyzed auto-tandem reaction with hexamethylditin and 4-nitrobenzaldehyde at constant Pd-concentration. (d) Linear/branched product ratio of this coupling using different SCS-pincer Pd-complexes.

We believe that these small effects can be explained by taking the solubility and the conformational behavior of the dendritic supports into account. These considerations lead us to propose that under the reaction conditions dendrimer

aggregation takes place for the carbosilane dendrimers and peripheral group backfolding occurs in PAMAM dendrimers, which lead to the observed catalytic behavior of the dendritic catalysts.

The apolar carbosilane catalysts are soluble in the dichloromethane/methanol (9 : 1, v/v) solvent mixture, which may be considered as rather polar on the basis of the dielectric constants of these solvents (ε = 9.1 for CH_2Cl_2, and 33 for CH_3OH). It is known that the introduction of apolar polymers into polar solvents leads to polymer entanglement. In this way, macroscopic clusters of these polymeric materials are formed in order to minimize the Gibbs free energy of the mixture.[39,40] These materials show a tendency to self-assembly into clusters that are solvated by the least polar solvent system, dichloromethane in our case. From the catalytic point of view, the accumulation of dendritic catalysts by means of self-assembled clusters is likely to lead to a decreased number of accessible catalyst sites, and therefore a lower reaction rate for the cross-coupling reaction catalyzed by the CS-based catalysts. For the polar PAMAM dendrimers no aggregation in the reaction medium is expected and therefore the observed reaction rates are comparable to those of monomeric catalysts.

The differences in product selectivity in the cross coupling reaction can be explained by the role of peripheral group backfolding. With respect to PAMAM dendrimers, carbosilane dendrimers are relatively small, rigid and sterically crowded. For this reason no backfolding of peripheral groups takes place for these type of dendrimers (see Elshakre *et al.*[22] for a structural study between carbosilane and PAMAM dendrimers). The observed selectivity of these carbosilane based catalysts is therefore similar to the tested monomeric catalysts: the catalysts on the outside of the self-assembled clusters possess a similar local reaction environment as the monomeric catalysts and accordingly lead to a similar product selectivity. At the same time, catalytic moieties located on the inside of a cluster are not reached by the substrates, and therefore do not take part in catalysis and hence do not affect product selectivity.

Because of the relatively long dendritic arms and the possibility to form hydrogen bonds, backfolding of the peripheral groups towards the interior of the PAMAM-dendrimers is a well-known phenomenon.[22,41–43] The peripheral catalysts that are brought closely to the crowded center of the dendrimer, are expected to experience a different and more crowded reaction environment than monomeric catalysts or peripherally located catalysts. In the catalytic cycle as published by Szabó,[29] the formation of the branched isomers takes place *via* a (direct) S_N2 attack of a SCS-pincer Pd–vinyl intermediate on vinyl epoxide, whereas for the linear isomers in this step a (conjugated) S_N2' attack on vinyl epoxide occurs (Fig. 7). When steric crowding around the vinyl–Pd intermediate increases, the S_N2' attack on the terminal olefin of vinyl oxirane, *i.e.* the sterically least hindered reaction pathway, would be favoured. Accordingly, formation of the linear product isomer is even more favored than formation of the branched product isomer under backfolding conditions. This leads to an overall increase in the linear: branched product ratio, even though reaction kinetics are likely slower at a backfolding catalytic site.

For the auto-tandem reaction between cinnamyl chloride, hexamethylditin and 4-nitrobenzaldehyde (reaction 2) the differences in the reaction characteristics between the various catalysts were smaller than for the cross coupling reaction. The structural arguments for these differences, *i.e.* accumulation of apolar carbosilane dendrimers and backfolding of PAMAM dendrimers, still hold for the tandem reaction as it was carried out in the same solvent system, but do not seem to have a large impact on the reaction characteristics of this reaction. The most striking observation for this tandem reaction is the improved selectivity of the largest PAMAM-dendrimer **5** compared to all other tested catalysts. This positive dendritic effect might again be caused by increased steric crowding because of partial backfolding of the catalysts to the dendrimer interior. A closer look at the mechanism of the tandem reaction[38] shows that the SCS-pincer Pd-η^1-allyl intermediate attacks the electrophilic 4-nitrobenzaldehyde to form both *syn*- and *anti*-products (Fig. 8). The distinction between the formation of these products is the relative orientation of the two reaction partners in the transition state. Due to the large 4-nitrobenzyl-group, the orientation is always favored to a positioning that leads to an *anti*-product, since in all cases these diastereoisomers are observed in excess. In a sterically crowded environment, this effect is likely enhanced leading to a higher selectivity for dendritic catalyst **5**.

In conclusion, the role of the dendritic support in dendrimer-immobilized homogeneous catalysis has been investigated for a series of dendritic catalysts in which the dendritic backbone was varied. For one of the catalytic reactions that was studied the change in dendritic support had a clear effect, whereas for the other reaction the effect was minor. These observations indicate that the role of the dendritic support in 'directing' a catalytic reaction seems very much dependent on the specific reaction intrinsics. It would therefore be of interest to explore reactions that have been proven to show a positive dendritic effect with regards to selectivity or reaction rate, with entirely different dendritic scaffolds than in the original studies. Further studies, using either very apolar or very polar substrates might also enhance the observed effects that have been discussed here and

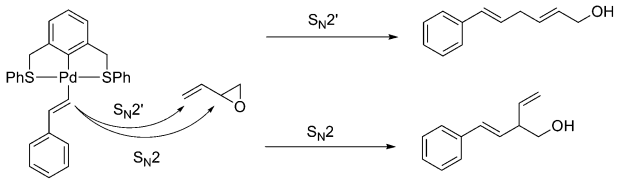

Fig. 7 The product formation step in the catalytic cycle of the cross-coupling as proposed by Szabó.[29]

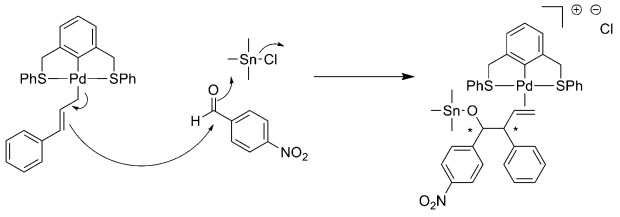

Fig. 8 The product formation step in the catalytic cycle of the cross-coupling as proposed by us.[38]

eventually might lead to a more rational choice of the dendrimer support to be used in homogeneous catalysts.

Experimental section

General

All reactions were carried out using standard Schlenk techniques under an inert dinitrogen atmosphere unless stated otherwise. All solvents were carefully dried and distilled prior to use. All standard reagents were purchased commercially and used without further purification. Compounds **9** (synthesis described by Amijs *et al.*,[32] analytical data present in Paugam *et al.*),[44] **10**[33] and $[Pd(MeCN)_4](BF_4)_2$[45] were prepared according to literature procedures. The PAMAM dendrimers were purchased by Dendritech as solutions in MeOH (G_0: 39.36% w/w, G_1: 45.10% w/w, G_2: 30.17% w/w) and used as received. All other reagents were purchased from Acros Organics and Sigma-Aldrich Chemical Co. Inc. and used as received. ^{1}H (300 MHz) and ^{13}C (100 MHz) NMR spectra were recorded on Varian spectrometers at 25 °C, chemical shifts are given in ppm referenced to residual solvent resonances. UV-Vis spectra were recorded on a Cary 50 Scan UV-visible spectrophotometer. IR spectra (ATR) were measured with a Perkin Elmer Spectrum One FT-IR instrument. High resolution mass spectroscopy (HRMS) has been performed on a Waters LCT Premier XE Micromass instrument using the electrospray ionization technique.

Syntheses

3,5-Bis(phenylsulfidomethyl)benzoic acid 11. To a cooled solution (−80 °C) of 3,5-bis(phenylthiomethyl)bromobenzene (**10**, 2.00 g, 4.98 mmol) in Et_2O (60 mL) was added a 1.6 M *t*BuLi solution in hexanes (2.0 equiv., 6.23 mmol, 9.97 mL). The resulting yellow mixture was stirred for 5 min. Then, dry CO_2 (large excess) was bubbled through the solution. Immediately a white precipitation was formed. The suspension was allowed to reach room temperature and water (1 mL) was added resulting in a clear solution. Then, the volatiles were removed and the resulting slurry was taken up in dichloromethane (100 mL) and extracted with an aqueous 4 M HCl solution (3 × 100 mL). The organic fractions were collected and evaporated *in vacuo*. The resulting syrup was redissolved in CH_2Cl_2 (3 mL) and precipitated by slow addition of hexanes. The supernatant was removed to yield a white powder (1.30 g, 71%).

^{1}H NMR (DMSO-d_6, 300 MHz): δ 13.02 (bs, 1H, COOH), 7.79 (s, 2H, ArH), 7.61 (s, 1H, ArH), 7.32–7.21 (m, 6H, *m*,*p*-SPh), 7.19–7.16 (m, 4H, *o*-SPh), 4.28 (s, 4H, CH_2). ^{13}C NMR (DMSO-d_6, 100 MHz) δ 167.6, 139.1, 136.2, 134.2, 131.6, 129.7, 129.3, 129.1, 126.8, 36.9. IR (ATR): ν_{OH} 2605 cm^{-1}, ν_{CO} 1687 cm^{-1}. ESI-HRMS for $C_{21}H_{18}O_2S_2$ (*m*/*z*): [M + Na$^+$] 389.0667 (calc. 389.0646).

2,5-Dioxopyrrolidin-1-yl-3,5-bis(phenylthiomethyl)benzoate 12. Benzoic acid **11** (1.00 g, 2.97 mmol) was dissolved in dichloromethane (40 mL). Subsequently triethylamine (1.2 equiv., 0.50 mL, 3.57 mmol), 1-ethyl-3-(3-dimethylaminopropyl)carbodiimide (EDC, 1.2 equiv., 0.68 g, 3.57 mmol) and *N*-hydroxysuccinimide (1.2 equiv., 0.41 g, 3.57 mmol) were added to the solution and the reaction mixture was stirred for 16 h. Water (40 mL) was added to the reaction and the resulting biphasic solution was extracted with water (4 × 40 mL) to get rid of the formed urea product. The product was purified *via* column chromatography (hexanes: THF 2 : 1 v/v) resulting in a white powder (1.09 g, 80%).

^{1}H NMR ($CDCl_3$, 300 MHz): δ 7.86 (s, 2H, ArH), 7.47 (s, 1H, ArH), 7.30–7.17 (m, 10H, SPh), 4.05 (s, 4H, SCH_2), 2.87 (s, 4H, C(=O)CH_2). ^{13}C NMR ($CDCl_3$, 100 MHz) δ 164.7, 156.9, 134.6, 131.1, 130.6, 126.1, 125.3, 124.8, 122.5, 120.9, 34.2, 21.2. ESI-HRMS for $C_{25}H_{21}NO_4S_2$ (*m*/*z*): [M + Na]$^+$ 486.0829 (calc. 486.0810).

SCS-pincer Pd-complex 13. To a solution of SCS-pincer ligand **12** (1.36 g, 2.93 mmol) in acetonitrile (40 mL) was added $[Pd(MeCN)_4](BF_4)_2$ (1.1 equiv., 1.43 g, 3.23 mmol). The yellow solution was stirred for 16 h at reflux temperature, whereupon the solvent was evaporated. Subsequently, the resulting solids were suspended by adding acetone (40 mL). NaCl (large excess) was added and the suspension was stirred for 1 h. The reaction mixture was filtered and the volatiles were removed *in vacuo*. The resulting solids were redissolved in CH_2Cl_2 (50 mL) and extracted with water (50 mL). The organic fractions were dried over $MgSO_4$, filtered and treated with polyvinylpyridine (PVPy; approximately 100 equiv.) to scavenge eventual present Pd(0) impurities. The PVPy was removed by filtration and the resulting clear solution was concentrated. The product slowly precipitates from the solution and was collected by decantation of the supernatant. This solution was concentrated and the precipitated product was collected again. This cycle was repeated five times. The solid fractions were collected and yielded 1.38 g (78%) of a pale yellow powder.

^{1}H NMR (CD_2Cl_2, 300 MHz): δ 7.79–7.72 (m, 6H, *o*-SPh + ArH), 7.43–7.37 (m, 6H, *m*,*p*-SPh), 4.70 (bs, 4H, SCH_2), 2.84 (s, 4H, C(=O)CH_2). ^{13}C NMR (CD_2Cl_2, 100 MHz) δ 169.5, 162.1, 150.8, 132.1, 131.6, 130.4, 130.0, 129.9, 123.6, 121.8, 52.5, 25.9. ESI-HRMS for $C_{25}H_{20}ClNO_4PdS_2$ (*m*/*z*): [2M − Cl]$^+$ = 1172.9449 (calc. = 1172.9440). UV/Vis (CH_2Cl_2): λ_{max} = 330.1 nm.

SCS-pincer Pd-complex 2. Active ester complex **13** (28.3 mg, 46.9 μmol) and butylamine (1.0 equiv., 4.6 μL, 46.9 μmol) were dissolved in CH_2Cl_2 (2 mL). The reaction mixture was stirred for 2 h. After performing a ninhydrin test on a TLC plate to confirm that no primary amines were present in the solution,[36] the reaction was stopped by diluting it to 10 mL CH_2Cl_2 and a similar volume of water. This biphasic mixture was extracted and the organic phase was washed two more times with water and brine (2 × 10 mL). The organic fraction was dried over $MgSO_4$, filtered and concentrated *in vacuo* yielding a yellow solid (21.6 mg, 82%).

^{1}H NMR (CD_2Cl_2, 300 MHz): δ 7.85 (m, 4H, *o*-SPh), 7.47–7.43 (m, 8H, ArH + *m*,*p*-SPh), 6.39 (t, ^3J = 4.5 Hz, 1H, NH), 4.67 (bs, 4H, SCH_2), 3.38 (q, ^3J = 6.9 Hz, 2H, NCH_2), 1.57 (m, 2H, NCH_2CH_2), 1.42 (m, 2H, CH_3CH_2), 0.97 (t, ^3J = 7.2 Hz, CH_3). ^{13}C NMR (CD_2Cl_2, 100 MHz) δ 174.2, 149.9, 132.2, 131.8, 130.2, 130.0, 129.9, 123.8, 120.8, 52.4, 40.1, 31.9, 20.4, 14.0. ESI-HRMS for $C_{25}H_{26}ClNOPdS_2$ (*m*/*z*): [M − Cl + MeCN]$^+$ = 567.0720 (calc. = 567.0765). UV/Vis (CH_2Cl_2): λ_{max} = 330.1 nm. IR (ATR): ν_{max} 3344 m, 3056 w, 2957 m, 2929 m, 2857 m, 1652 s, 1586 m,

1533 s, 1477 m, 1438 s, 1317 m, 1274 m, 1245 s, 1023 s, 902 m, 754 s, 740 s, 685 s.

Synthesis of dendritic catalysts 3, 4 and 5

General procedure. To a mixture of CH_2Cl_2 and MeOH (1 : 1 v/v; 10 mL) was added G_x-PAMAM-NH_2 dendrimer (solution in MeOH, purchased by Dendritech) and 1.25 equiv. of **13** per dendritic arm. This solution was stirred at room temperature. At regular intervals, a ninhydrin test on TLC was performed to check the remainder of primary amines in the solution.[36] The reaction was stopped when primary amines were no longer detected. The dendritic compound was purified by passive dialysis. To this end, the reaction mixture was concentrated to 5 mL and placed into a dialysis bag. This bag was placed into a beaker containing a mixture of CH_2Cl_2 : MeOH (200 mL; 1 : 1 v/v) and dialyzed for 2 h. This procedure was repeated twice. The contents of the dialysis bag were removed from the bag and evaporated to dryness to yield the PAMAM-G_x-(SCS-Pd-Cl)$_n$ materials.

PAMAM-G_0-(SCS-Pd-Cl)$_4$ 3. Yield: 110 mg (66%). ^{1}H NMR (CD_2Cl_2/CD_3OD 1 : 1): δ 7.77 (m, 16H, *o*-SPh), 7.45 (s, 8H, ArH), 7.38–7.32 (m, 24H, *m*,*p*-SPh), 4.60 (bs, 16H, SCH_2), 3.40–3.30 (m, 16H, $NHCH_2CH_2NH$), 2.62 (m, 8H, $NCH_2CH_2C(=O)$), 2.40 (s, 4H, NCH_2CH_2N), 2.26 (m, 8H, $NCH_2CH_2C(=O)$). ^{13}C NMR (CD_2Cl_2/CD_3OD 1 : 1) δ 173.9, 168.1, 150.0, 132.2, 131.7, 131.1, 130.3, 129.8, 129.1, 121.1, 52.4, 50.9, 49.9, 40.2, 39.1, 33.4. UV/Vis (CH_2Cl_2): λ_{max} = 330.1 nm. IR (ATR): ν_{max} = 3287 br, 3056 m, 2926 m, 2854 m, 1634 s, 1580 m, 1532 s, 1471 m, 1440 s, 1322 m, 1254 s, 1024 m, 908 m, 742 s, 685 s. ESI-HRMS for $C_{104}H_{108}Cl_4N_{12}O_8Pd_4S_8$ (*m*/*z*): $[M - 2Cl]^{2+}$ = 1201.0618 (calc. = 1201.0865).

PAMAM-G_1-(SCS-Pd-Cl)$_8$ 4. Yield: 140 mg (78%). ^{1}H NMR (CD_2Cl_2/CD_3OD 1 : 1): δ 7.79 (m, 32H, *o*-SPh), 7.48 (bs, 16H, ArH), 7.39 (m, 48H, *m*,*p*-SPh), 4.65 (bs, 32H, SCH_2), 3.44–3.16 (m, 32H, $NHCH_2CH_2NH$), 2.87 (m, 8H, $NHCH_2CH_2N$), 2.70 (m, 24H, $NCH_2CH_2C(=O)$), 2.48 (s, 12H, NCH_2CH_2N + $NHCH_2CH_2N$), 2.30 (m, 24H, $NCH_2CH_2C(=O)$). ^{13}C NMR (CD_2Cl_2/CD_3OD 1 : 1) δ 174.0, 170.0 (two signals), 150.1, 132.2, 131.6, 131.2, 130.2, 129.8 (two signals), 121.1, 52.3, 50.0 (two signals), 49.2 (two signals), 40.1, 39.1, 37.6, 33.7. UV/Vis (CH_2Cl_2): λ_{max} = 330.1 nm. IR (ATR): ν_{max} = 3287 br, 3053 m, 2934 m, 2823 m, 1635 s, 1580 m, 1526 s, 1471 m, 1440 s, 1320 m, 1251 s, 1024 m, 907 m, 740 s, 685 s.

PAMAM-G_2-(SCS-Pd-Cl)$_{16}$ 5. Yield: 140 mg (77%). ^{1}H NMR (CD_2Cl_2/CD_3OD 1 : 1): δ 7.76 (m, 64H, *o*-SPh), 7.47 (bs, 32H, ArH), 7.36 (m, 96H, *m*,*p*-SPh), 4.63 (bs, 64H, SCH_2), 3.40–3.16 (m, 64H, $NHCH_2CH_2NH$), 2.87 (m, 24H, $NHCH_2CH_2N$), 2.68 (m, 56H, $NCH_2CH_2C(=O)$), 2.48 (bs, 28H, NCH_2CH_2N + $NHCH_2CH_2N$), 2.28 (m, 56H, $NCH_2CH_2C(=O)$). ^{13}C NMR (CD_2Cl_2/CD_3OD 1 : 1) δ 174.1, 168.1 (three signals), 150.1, 132.0, 131.8, 131.2, 130.3, 129.8 (two signals), 121.2, 52.4, 50.1 (three signals), 49.3 (three signals), 40.2 (two signals), 39.1, 37.6, 33.8 (three signals). UV/Vis (CH_2Cl_2): λ_{max} = 330.1 nm. IR (ATR) ν_{max} = 3287 br, 3059 m, 2965 m, 2926 m, 1634 s, 1580 m, 1532 s, 1470 m, 1440 s, 1323 m, 1253 s, 1024 m, 908 m, 742 s, 686 m.

General protocol for the cross coupling of vinyl epoxide with phenylvinylboronic acid. A catalyst solution (2 mol% Pd, 0.016 mmol Pd centers) in a mixture of CH_2Cl_2 and MeOH (9 : 1 v/v, 2 mL) was added to a solution of vinyl epoxide (1.0 equiv., 0.80 mmol, 64 μL), phenylvinylboronic acid (1.0 equiv., 0.80 mmol, 118.4 mg), Cs_2CO_3 (2.0 equiv., 1.6 mmol, 521 mg), and hexamethylbenzene (internal standard, 0.111 mmol, 14.4 mg) in a mixture of CH_2Cl_2 and MeOH (9 : 1 v/v, 18 mL). The reaction mixture was stirred at room temperature in a nitrogen environment. Aliquots of 50 μL for NMR/GC analysis were taken at regular time intervals with an airtight syringe.

General protocol for the stannylation/electrophilic addition tandem reaction. A catalyst solution (2 mol% Pd, 0.016 mmol Pd centers) in a mixture of CH_2Cl_2 and MeOH (9 : 1 v/v, 2 mL) was added to a solution of cinnamyl chloride (3.0 equiv., 2.40 mmol, 0.34 mL), hexamethylditin (3.0 equiv., 2.40 mmol, 0.50 mL), 4-nitrobenzaldehyde (1.0 equiv., 0.80 mmol, 121 mg), and hexamethylbenzene (internal standard, 0.088 mmol, 14.4 mg) in a mixture of CH_2Cl_2 and MeOH (9 : 1 v/v, 10 mL). The reaction stirred at room temperature in a nitrogen environment. Aliquots of 50 μL for NMR/GC analysis were taken at regular time intervals with an airtight syringe.

References

1 H. P. Dijkstra, G. P. M. van Klink and G. van Koten, *Acc. Chem. Res.*, 2002, **35**, 798–810.
2 J. W. J. Knapen, A. W. van der Made, J. C. de Wilde, P. W. N. M. van Leeuwen, P. Wijkens, D. M. Grove and G. van Koten, *Nature*, 1994, **372**, 659–663.
3 D. Astruc and F. Chardac, *Chem. Rev.*, 2001, **101**, 2991–3023.
4 R. Kreiter, A. W. Kleij, R. J. M. Klein Gebbink and G. van Koten, *Top. Curr. Chem.*, 2001, **217**, 163–199.
5 P. A. Chase, R. J. M. Klein Gebbink and G. van Koten, *J. Organomet. Chem.*, 2004, **689**, 4016–4054.
6 J. K. Kassube and L. H. Gade, *Top. Organomet. Chem.*, 2006, **20**(Dendrimer Catal), 39–59.
7 A. Berger, R. J. M. Klein Gebbink and G. van Koten, *Top. Organomet. Chem.*, 2006, **20**(Dendrimer Catal.), 1–38.
8 R. Andres, E. de Jesús and J. C. Flores, *New J. Chem.*, 2007, **31**, 1161–1191.
9 B. Helms and J. M. J. Fréchet, *Adv. Synth. Catal.*, 2006, **348**, 1125–1148.
10 A. W. Bosman, H. M. Janssen and E. W. Meijer, *Chem. Rev.*, 1999, **99**, 1665–1688.
11 S. Gatard, S. Kahlal, D. Mery, S. Nlate, E. Cloutet, J. Y. Saillard and D. Astruc, *Organometallics*, 2004, **23**, 1313–1324.
12 J. L. Zhang, H. B. Zhou, J. S. Huang and C. M. Che, *Chem.–Eur. J.*, 2002, **8**, 1554–1562.
13 J. M. Benito, E. de Jesús, F. J. de la Mata, J. C. Flores and R. Gomez, *Chem. Commun.*, 2005, 5217–5219.
14 L. Ropartz, K. J. Haxton, D. F. Foster, R. E. Morris, A. M. Z. Slawin and D. J. Cole-Hamilton, *J. Chem. Soc., Dalton Trans.*, 2002, 4323–4334.
15 Y. Ribourdouille, G. D. Engel, M. Richard-Plouet and L. H. Gade, *Chem. Commun.*, 2003, 1228–1229.
16 A. Dahan and M. Portnoy, *Org. Lett.*, 2003, **5**, 1197–1200.
17 P. Servin, R. Laurent, L. Gonsalvi, M. Tristany, M. Peruzzini, J. P. Majoral and A. M. Caminade, *Dalton Trans.*, 2009, 4432–4434.
18 D. J. M. Snelders, G. van Koten and R. J. M. Klein Gebbink, *J. Am. Chem. Soc.*, 2009, **131**, 11407–11416.
19 A. W. Kleij, R. A. Gossage, R. J. M. Klein Gebbink, N. Brinkmann, E. J. Reijerse, U. Kragl, M. Lutz, A. L. Spek and G. van Koten, *J. Am. Chem. Soc.*, 2000, **122**, 12112–12124.

20 R. Breinbauer and E. N. Jacobsen, *Angew. Chem., Int. Ed.*, 2000, **39**, 3604–3607.
21 J. K. Kassube and L. H. Gade, *Adv. Synth. Catal.*, 2009, **351**, 739–749.
22 M. Elshakre, A. S. Atallah, S. Santos and S. Grigoras, *Comput. Theor. Polym. Sci.*, 2000, **10**, 21–28.
23 D. A. Tomalia, A. M. Naylor and W. A. Goddard, *Angew. Chem., Int. Ed. Engl.*, 1990, **29**, 138–175.
24 M. Labieniec and C. Watala, *Cent. Eur. J. Biol.*, 2009, **4**, 434–451.
25 R. Esfand and D. A. Tomalia, *Drug Discovery Today*, 2001, **6**, 427–436.
26 H. Frey and C. Schlenk, *Top. Curr. Chem.*, 2000, **210**, 69–129.
27 G. van Koten and J. T. B. H. Jastrzebski, *J. Mol. Catal. A: Chem.*, 1999, **146**, 317–323.
28 A. W. van der Made and P. W. N. M. van Leeuwen, *J. Chem. Soc., Chem. Commun.*, 1992, 1400–1401.
29 J. Kjellgren, J. Aydin, O. A. Wallner, I. V. Saltanova and K. J. Szabó, *Chem.–Eur. J.*, 2005, **11**, 5260–5268.
30 M. Gagliardo, N. Selander, N. C. Mehendale, G. van Koten, R. J. M. Klein Gebbink and K. J. Szabó, *Chem.–Eur. J.*, 2008, **14**, 4800–4809.
31 B. M. J. M. Suijkerbuijk, M. Q. Slagt, R. J. M. Klein Gebbink, M. Lutz, A. L. Spek and G. van Koten, *Tetrahedron Lett.*, 2002, **43**, 6565–6568.
32 C. H. M. Amijs, G. P. M. van Klink and G. van Koten, *Green Chem.*, 2003, **5**, 470–474.
33 M. D. Meijer, B. Mulder, G. P. M. van Klink and G. van Koten, *Inorg. Chim. Acta*, 2003, **352**, 247–252.
34 M. Q. Slagt, R. J. M. Klein Gebbink, M. Lutz, A. L. Spek and G. van Koten, *J. Chem. Soc., Dalton Trans.*, 2002, 2591–2592.
35 N. J. M. Pijnenburg, H. P. Dijkstra, G. van Koten and R. J. M. Klein Gebbink, *Dalton Trans.*, 2011, DOI: 10.1039/c1dt10502g.
36 E. Kaiser, R. L. Colescot, C. D. Bossinge and P. L. Cook, *Anal. Biochem.*, 1970, **34**, 595–605.
37 S. Bonnet, M. Lutz, A. L. Spek, G. van Koten and R. J. M. Klein Gebbink, *Organometallics*, 2010, **29**, 1157–1167.
38 N. J. M. Pijnenburg, Y. H. M. Cabon, G. van Koten and R. J. M. Klein Gebbink, manuscript in preparation.
39 A. Ravve, *Principles of Polymer Chemistry*, 2nd edn, Kluwer Academic, New York, 2000.
40 D. M. Teegarden, *Polymer Chemistry: Introduction to an Indispensable Science*, NSTA, Arlington, Virginia, 2004.
41 U. Boas, J. B. Christensen and P. M. H. Heegaard, *J. Mater. Chem.*, 2006, **16**, 3786–3798.
42 A. W. Opitz and N. J. Wagner, *J. Polym. Sci., Part B: Polym. Phys.*, 2006, **44**, 3062–3077.
43 M. Ballauff and C. N. Likos, *Angew. Chem., Int. Ed.*, 2004, **43**, 2998–3020.
44 M. F. Paugam, J. T. Bien, B. D. Smith, L. A. J. Chrisstoffels, F. de Jong and D. N. Reinhoudt, *J. Am. Chem. Soc.*, 1996, **118**, 9820–9825.
45 T. W. Lai and A. Sen, *Organometallics*, 1984, **3**, 866.